
Article:
Rees, SJ and Haves, P (2013) An experimental study of air flow and temperature distribution in a room with displacement ventilation and a chilled ceiling. Building and Environment, 59. pp. 358-368. ISSN: 0360-1323

https://doi.org/10.1016/j.buildenv.2012.09.001

An Experimental Study of Air Flow and Temperature Distribution in a Room with Displacement Ventilation and a Chilled Ceiling

Simon J. Rees[a,*], Philip Haves[b]

[a]*Institute of Energy and Sustainable Development, De Montfort University, The Gateway, Leicester, LE1 9BH, UK.*
[b]*Building Technologies, Lawrence Berkeley National Laboratory, 1 Cyclotron Road, MS 90R3111,Berkeley, CA 94720. USA.*

Abstract

Displacement ventilation and chilled ceiling panel systems are potentially more energy efficient than conventional air conditioning systems and are characterized by the presence of vertical temperature gradients and significant radiant asymmetry. The characteristics of this type of system have been studied by making temperature and air flow measurements in a test chamber over a range of operating parameters typical of office applications. Results from the displacement ventilation study are consistent with other studies and show that normalized temperature profiles are independent of internal heat gain. Linear temperature gradients in the lower part of the room were found, in all cases, to be driven by convection from the adjacent walls. Significant mixing, indicated by reduced temperature gradients, was evident in the upper part of the room in the chilled ceiling results at higher levels of heat gain. Visualization experiments, velocity measurements and related numerical studies indicated that with greater heat gains the plumes have sufficient momentum to drive flow across the ceiling surface and down the walls. The significance of forced, as opposed to natural convection, is also suggested by relatively low Richardson Number (Ri) values found near the ceiling. Furthermore, in cases with moderately high internal gains, comparison of the temperature gradients indicated that the effect of ceiling surface temperature on the degree of mixing and the magnitude of the temperature gradient were of secondary importance. These findings are in contrast to the view that it is natural convection at the ceiling that causes enhanced mixing.

Keywords: Displacement Ventilation, Chilled Ceiling, Convection, Room Heat Transfer, Air Distribution

1. Introduction

Displacement ventilation has been used in Northern Europe to provide cooling and ventilation in office spaces for more than two decades [1–3]. Although displacement ventilation has potential to provide lower draught risk, higher air quality and lower energy consumption when compared to conventional all-air cooling systems it has the disadvantage of only being able to deal with moderate cooling loads. Using displacement ventilation and chilled ceiling technologies [4–6] together so that ventilation is provided by displacement ventilation and larger sensible cooling loads can be dealt with by a chilled ceiling [7–9] is now regarded as a conventional design option in commercial office projects [10–12].

In displacement ventilation systems, air is introduced into the room near the floor at very low velocity and at a temperature that is only a few degrees below the effective temperature experienced by the occupants. The Reynolds number at the diffuser is at least one order of magnitude lower ($\sim$ 3800 in these experiments), and the Archimedes number significantly higher (typically 0.2-2), than in conventional jet-driven air distribution systems. As a result, the cool supply air descends towards, and spreads across, the floor in a gravity current [13, 14] and is slightly heated as it passes over the floor surface. Buoyant plumes are developed around any warm objects in the room, such as people and electrical equipment. Each plume increases in width as it rises and entrains more air from the surrounding cooler air. This warm (and contaminated) air rises until it reaches an upper zone bounded by the ceiling [15]. Accordingly, the room air distribution can be conceived of as a lower cooler zone, where conditions are close to that of the supply, and an upper zone of warm contaminated air that has been transported by the plumes. In steady state, the height of the boundary between these two zones (sometimes referred to as the 'stationary front') is defined by the height at which the flow rate in the plumes equals the supply flow rate [16].

The effect of the transport of heat to a layer of warm air near the ceiling is to produce a temperature gradient over most of the height of the room. There is a relationship between the air temperature gradient and thermal discomfort. Standards such as ASHRAE Standard 55-2010 [17] suggest a maximum overall head-to-foot difference of 3 K for acceptable thermal comfort. This could be interpreted as an allowable gradient of 2-3 K/m depending on if objects are considered seated or standing. To stay within these guidelines accordingly imposes a limit on the magnitude of the cooling load that can be met by displacement ventilation systems; values between 20 and 40 W/m^2 are suggested in the literature. It is this limitation that is addressed by combining displacement ventilation with chilled ceilings in order to achieve the capacities demanded in many office appli-

*Corresponding author. Tel.: +44 (0)116 2577974; fax: +44 (0)116 2577977

Email address: sjrees@dmu.ac.uk (Simon J. Rees)

cations. In this study, heat gain intensities up to 72 W/m^2 have been studied experimentally and this is representative of design levels for displacement ventilation combined with chilled ceilings although not quite as high as the maximum design values suggested elsewhere [8, 18].

Although there are a significant number of studies of displacement ventilation reported, there are relatively few that have been concerned with this form of ventilation combined with chilled ceilings. A limited set of vertical temperature distribution data for rooms using chilled ceiling panels and displacement ventilation were reported by Skåret [15], Behne [19], Krühne [20], Külpmann [21] and Alamdari [8]. These early studies show reduced temperature gradients compared to displacement ventilation alone, and in some cases, only small deviations from the average room temperature. Behne carried out more extensive measurements later[18] and we comment on this work below.

A number of fluid flow features found in these systems, such as inlet and plume flows, are common to purely displacement ventilation but also certain forms of natural ventilation [22] and are of some relevance to this study. Magnier *et al.* [14] have studied inlet conditions and those near the floor in some detail and verified the similarity to gravity current conditions. Theoretical studies of natural ventilation have been concerned with plume growth and the development of the upper warm layer dividing the room at the horizontal stationary front in both steady state [23, 24] and transient conditions [25]. Although such studies, and related physical modelling studies, consider the development of the upper warm layer adjacent the ceiling they do not consider ceiling heat transfer conditions. Theoretical models have been developed for situations with a chilled ceiling [26, 27] but make assumptions about heat transfer coefficients and turbulent conditions at the ceiling.

The characteristics of plumes, particularly those around the human body, are of general interest in ventilation flows and the development of breathing thermal manikins has enabled detailed measurements to be made. Such measurements have been reported recently by Zukowska *et al.* [28, 29] and Rim *et al.* [30]. They point out the sensitivity of the plume to features such as hair, clothing and chair shape, the slightly unsymmetric nature of plumes from seated persons and also the influence of the breathing process. Similar detailed study of plumes from office equipment have not been reported to date.

A few studies have been made of convection heat transfer conditions in rooms with displacement ventilation and chilled ceilings. The work reported by Novoselac *et al.* [31] was mostly concerned with floor heat transfer in rooms with displacement ventilation alone—the floor gravity current being rather different to that in other forms of mechanical ventilation. The studies by Jeong *et al.* [32] examined existing correlations for ceilings and the study by Karadağ [33] was based on numerical convection heat transfer results and theoretical radiant heat transfer models rather than experimental measurements. Andrés-Chicote *et al.* made an experimental study of convection from a chilled ceiling in a full size test room but without any plume heat sources. Causone *et al.* [34] also carried out full scale experiments in an unventilated test chamber. They comment on some systematic differences in measured ceiling convection coefficients when compared to other work and suggest this may be due to different reference temperature definitions but they also point out some systematic differences between cases with heated walls as the heat source and cases with plume heat sources. The physical modelling study by Thomas *et al.* [35], which employed an unventilated heated water tank with a small plume, did not quantify convection heat transfer coefficients but did highlight the existence of Rayleigh-Bérnard type convection cells close to the ceiling surface under steady state conditions. These cells seem to have been confined to a relatively shallow layer next to the ceiling surface and not induced large scale mixing in the upper part of the room. The authors suggest further experiments to investigate to what extent the Rayleigh-Bérnard cells at the surface would be influenced by other features or turbulent structures in the flow.

A concern that has often been commented upon is that the air quality (ventilation effectiveness) benefits of displacement ventilation may be negated, in part, by additional recirculation induced by any chilled ceiling. Krühne [20] reported some detrimental effects when the chilled ceiling carried some of the thermal load but these experiments were with relatively low heat gains (~20 W/m^2). Behne [18, 19] has carried out a more comprehensive study using tracer gas and temperature profile measurements. It was shown that temperature gradients were small and ventilation effectiveness close to unity in the upper part of the room when the chilled ceiling operated and that conditions in the lower part of the room also varied depending on how much load was apportioned to the chilled ceiling. Three reasons were suggested for the increased recirculation and reduced air quality:

(i) natural convective cooling at the ceiling surface causing the air to fall and mix with the air below;

(ii) radiant heat exchange causing cooling of the upper walls and so inducing negatively buoyant wall jets;

(iii) buoyant flow in the rising plumes being of greater volume flow rate than that supplied by the displacement ventilation system.

Behne [18] acknowledges that these possible effects are interrelated and so "it is hard to tell which influences or causes the other". It was suggested that a good design metric was the proportion of the load shared by the chilled ceiling system—higher values indicating smaller temperature gradients but more mixing and so poorer air quality—and this suggests lower ceiling temperatures are responsible for the increased recirculation. This idea was endorsed in [10] and design charts proposed on this basis. However, the cause and effect relationship between the proportion of load carried by the ceiling and the degree of mixing is not clear. In particular, the division of the load between the air and radiant systems depends not just on ceiling temperature but also on the air flow rate. The air flow rate, as well as the number and strength of the plumes in the room, are directly related to the position of the stationary front. The stationary front, and hence size of the upper mixed air layer,

is determined according to the requirement for conservation of mass and does not depend directly on heat transfer processes [23]. The reason for the impaired air quality, relative to pure displacement ventilation, is often stated (e.g. [8]) to be the first of those given by Behne; natural convection and negative buoyancy driven by the cool ceiling surface. We address this question later.

The experiments reported here were carried out as part of a project to develop a nodal model of displacement ventilation and chilled ceiling systems for use in annual energy simulation [36]. The nodal model in question required detailed measurements of air and surface temperatures over a range of operating conditions for the calculation of its parameters. To this end, it was necessary to carry out a series of environmental test chamber experiments. These experiments, in addition to providing the necessary data for model development, have also allowed the study of the operating characteristics of displacement ventilation systems used with and without chilled ceilings. The same test chamber has been used for thermal comfort studies reported elsewhere [37, 38].

The results of the experiments are presented here firstly in the form of vertical air temperature distributions. Because of the sensitive nature of the coupling of the room airflow and temperature distributions, the vertical air temperature profiles are particularly informative. In particular, the shape of the temperature profile indicates the degree of mixing at different levels in the room—lower temperature gradients being indicative of grater mixing. We present and discus the experimental results in three sections of this paper. Results are presented firstly for cases where the displacement ventilation system was operated on its own and these cases are those with modest heat gains. Secondly, results characterising the combined operation of the displacement ventilation and chilled ceiling are presented. Finally, we discuss the mixing conditions in the upper part of the room—and the nature of the convective heat transfer at the ceiling surface in particular—in more detail in a further section of the paper.

Results with displacement ventilation alone are included to allow some distinctions to be made between passive surface behavior and the effect of the chilled ceiling. Air velocity data are also presented and comparisons made with CFD calculations reported elsewhere [39]. Previous experimental studies have examined conditions based on air temperature profiles and tracer gas concentration profiles. Where velocity measurements have been made these have been concerned with the inlet [14] and plume conditions [28] rather than conditions near the ceiling. The inclusion of velocity measurements in this study has allowed convection conditions at the ceiling to be analysed in more detail so that some conclusions about the nature of the mixing processes can be made.

2. Description of the test chamber

The experiments reported here were conducted in a test chamber of a size representative of a two-person office, having internal dimensions of 5.43 m long, 3.08 m wide and 2.78 m high. The general arrangement is shown in Figs. 1 and 2. The displacement ventilation system air supply was via a semicylindrical diffuser 700 mm high and 400 mm diameter that is on the centerline of one of the shorter walls and has an open area estimated to be 80% of the geometric area. The ventilation system extract was via a 125 mm high and 575 mm long grille above the door. The chilled ceiling was constructed from a proprietary system of smooth metal tiles 1.65 m long and 0.3 m wide occupying 88% of the total ceiling area (this was the maximum active area that could be achieved after allowing space for the ceiling support system). The panels consisted of a serpentine array of tubes fixed to a perforated metal plate and in contact with the upper side of the metal tile. There was 125 mm of fiberglass insulation in the void above the array of tubes.

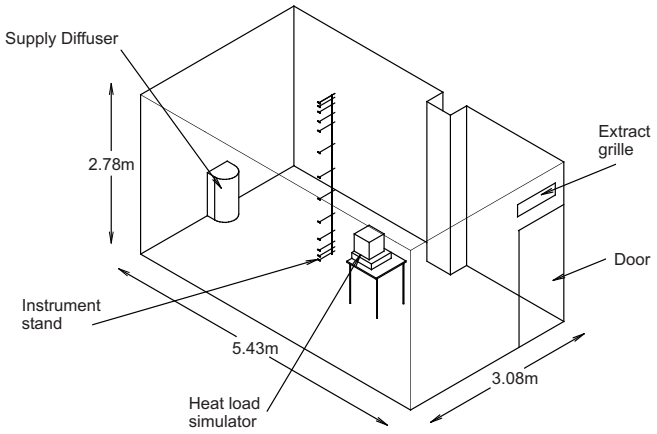

Figure 1: The configuration of the environmental test chamber.

The air supply for the displacement ventilation system was ducted from an air handling unit that included a direct expansion cooling coil, a thermistor-controlled electric heating element and a variable speed supply air fan. The temperature of the air stream could be controlled within a ±0.1 K band when the unit is in heating mode and within ±0.3 K in cooling mode. The air flow rates in the supply and extract streams were determined by using a fluorocarbon manometer to measure the pressure drop across a multi-hole orifice plate. This arrangement allowed the flow rate to be measured with an accuracy of ±0.9 l/s (±2.25% at the design flow rate).

Chilled water was supplied to the ceiling panel system from a central chilled water buffer tank. Using this arrangement the chilled ceiling water supply temperature could be controlled within a ±0.2 K band. The water flow rate was high enough to ensure a temperature difference of only 2–3 K across the chilled ceiling panel system at full load and so minimize any temperature difference across the ceiling surface.

The chamber is moderately well insulated and was originally designed so that wall internal surface temperatures could be closely controlled by hydronic radiant panels (visible in Fig. 2). The thermal conductances of the floor and ceiling were measured to be 0.64 $W/m^2.K$ and 0.41 $W/m^2.K$ respectively. The chamber walls were measured to have conductances between 0.34 $W/m^2.K$ and 1.7 $W/m^2.K$. Rather than control the wall sur-

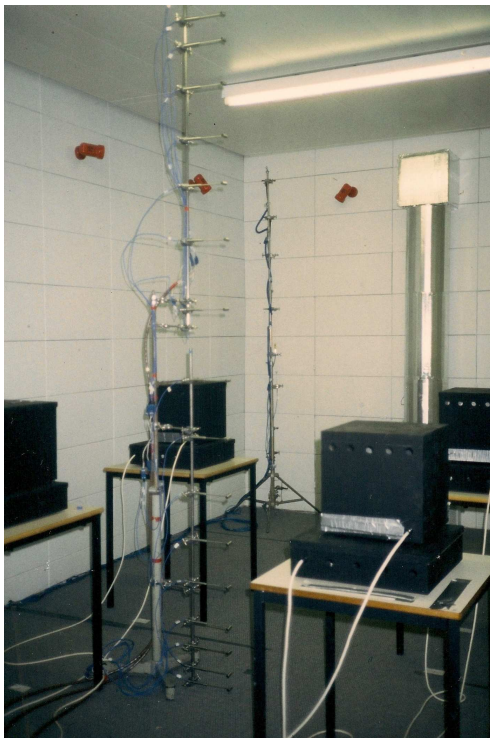

Figure 2: A photograph of the test chamber configured for 4 heat sources and showing the air temperature sensor assembly.

face temperatures, it was thought more realistic to allow the walls to behave passively so that temperature and heat flux gradients could develop in response to the room air temperature and radiant asymmetries in much the same way as a real office. This meant that conduction losses and gains were present; depending on the temperature in the surrounding laboratory space. Although the temperature in this space is not closely controlled it was stable and some adjustment in the conduction losses could be made by adjusting the absolute values of the displacement ventilation and chilled water supply temperatures. In the series of experiments reported here the lab was at a temperature close to the mean temperature of the test room and so the conduction losses are not significant. This is reflected in the small differences between the wall surface and room air temperatures reported below.

2.1. The measurement systems

The primary air and wall surface temperatures were measured with type 'T' copper-constantan thermocouples. The air temperature sensor thermocouple junction was contained within an open-ended stainless steel tube to give some shielding from long wave radiation. Up to eighteen sensors were mounted on a vertical stand to allow measurement of the room vertical temperature distribution Surface temperature thermocouples were distributed around the walls in seven vertical lines, each with four sensors, to allow measurement of vertical temperature profiles. Thirteen surface temperature sensors were installed on the chilled ceiling and six on the floor surface. There were additional thermocouples on the outer surfaces of the test chamber, giving a total of 51 surface temperature measurement locations. In each experiment the test chamber was operated with the supply temperatures and heat gains fixed at the desired level for approximately 8 hours to ensure stable conditions were obtained (surface and air temperatures changing no more than a fraction of a degree per hour). All temperature data have been derived from measurements averaged over a 30–40 minute period.

The signal processing and data logging system for the thermocouples was constructed using data acquisition cards designed for use with a personal computer based data logging system. Cold temperature compensation on the data acquisition cards proved unsatisfactory and so an ice reference point was used for each group of thermocouples. Testing of this ice-point-based measurement system before and after the experiments using an in-situ calibration procedure showed the air thermocouple measurements to be repeatable to ±0.17 K (absolute) and the surface temperature to air temperature difference measurements to be repeatable to ±0.25 K. Further details of the calibration procedures are given in [40].

A limited series of velocity measurements were made in the test chamber using a multi-channel Constant Temperature Anemometry system [41] with 12 sensors. The airflow transducer used in this system is a combined omni-directional velocity (speed) and temperature sensor designed specifically for measuring room airflows within the velocity range 0.05–5.0 m/s. The sensors have a nominal accuracy of ±0.01 m/s (±5%) but after correcting the readings according to individual calibration data an accuracy of ±2% could be expected [42]. The air flow transducers were mounted on the same vertical stand as the room air thermocouples and were more closely spaced near the floor and ceiling. In one of the experiments, measurements were made at a number of positions along the centerline of the room. These positions are shown in Fig.3.

Internal heat gains were simulated using two sizes of cuboid boxes containing incandescent light bulbs of various wattages. The boxes were painted matt black and had a series of ventilation holes around the sides to allow some airflow through the box by natural convection. When stacked, these boxes were intended to simulate a personal computer and monitor and were placed on top of 600 mm square tables at a height of 720 mm. The heat sources were distributed in the test chamber in one of two plan layouts. For cases with small loads, a single set of boxes was placed on a table on the centerline of the room. For test cases with larger total heat gains, four sets of boxes were placed on tables set symmetrically about the room centerline, as illustrated in Fig.3.

The size of the internal loads simulated varied from 100 W in a single box, up to 1200 W distributed equally in four boxes. These loads are equivalent to 6-72 W/m^2 normalized by floor area. The radiant component of the heat output from the load simulator boxes was measured as 50-55% by taking a series of radiometer readings over the box surfaces. The arrangement of the loads and air temperature measuring positions is shown in Fig.3. Air temperature measurements were made at either point A where a single heat source was used, or point B where four heat sources were used, unless otherwise stated.

The heat sources are intended to be representative of desk-

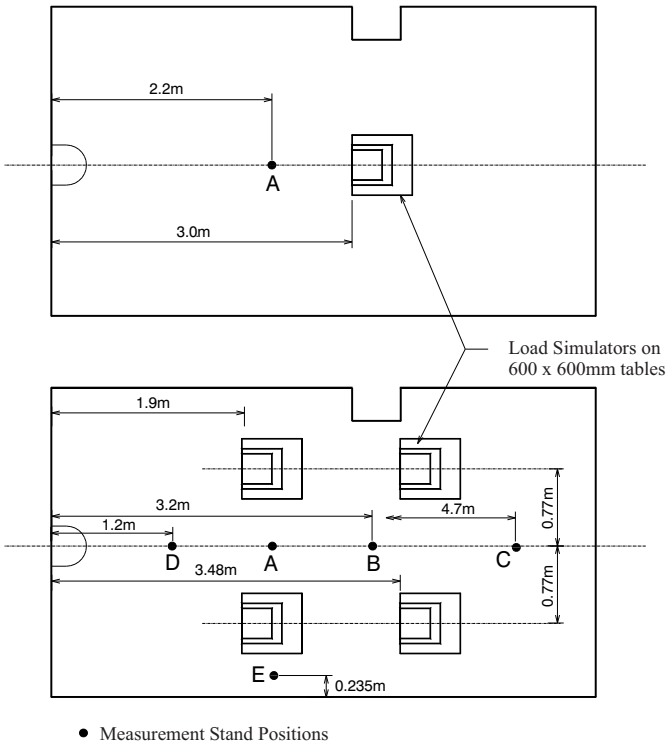

Figure 3: Plan views of the test chamber showing the layout of the room with single and four load simulator boxes and showing temperature and velocity measurement locations A to E.

top computing equipment and these were thought to be the most significant type in offices where displacement ventilation and chilled ceiling systems might be applied. In real office conditions heat sources vary in form and clearly additional plumes associated with occupants would be present. Seated occupants would produce plumes that started lower in the room and be slightly unsymmetric [29]. Head height would be similar to the top of the heat sources used here. Although occupant simulators were not available, the same test chamber and table arrangement was used for a related comfort study with human test subjects [38]. The temperature profiles were found to be very similar in nature to those reported here using artificial heat sources.

3. Displacement ventilation characteristics

Test chamber experiments were carried out for twelve cases using the displacement ventilation system without any cooling from the chilled ceiling. These were made with a number of different size heat gains (Q) in the range 100–400 W (6–24 W/m^2) and room air change rates of 1.5 and 3.0 per hour. In this section, we characterize the behavior of the displacement ventilation system in terms of the air and wall temperature profiles and the vertical radiant exchange.

The air (T_a) and wall temperature (T_w) profiles for the displacement ventilation test cases with a supply air flow equivalent to 1.5 air changes per hour are shown in Fig. 4. The results for the test cases with a supply air change rate of 3.0 per hour are shown in Fig. 5. To make comparisons between different experiments, the temperatures in these figures are normalized to the supply air temperature (T_s). Only small lateral variations were observed in the wall surface temperature and so the wall temperature profiles shown are the area-weighted average of the measurements at each of four heights (there being seven sensors at each height). The average floor and ceiling surface temperatures are shown as points on the bottom and top horizontal axis of these figures respectively. The air temperature profiles were measured on the room centerline at the position marked as point A (Fig. 3) for the results using a single heat source in Fig. 4 and point B for those using four heat sources in Fig. 5.

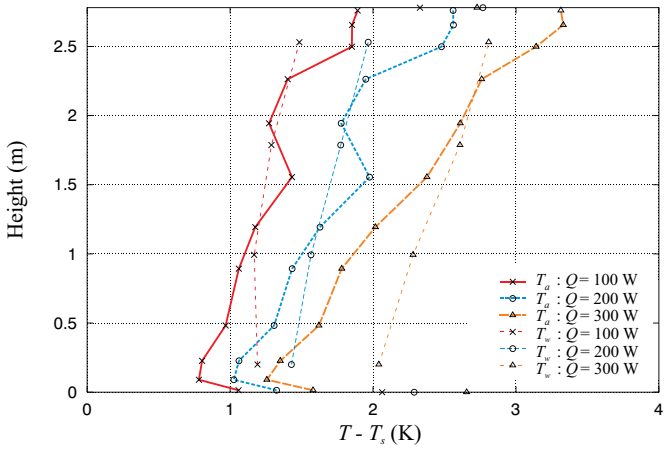

Figure 4: Air (T_a) and wall surface temperature (T_w) distributions for displacement ventilation under different heat gain conditions (Q=100–300 W) and an air change rate of 1.5 per hour.

There are a number of features of the air temperature profiles that can be seen to be common to these displacement ventilation test cases. Firstly, there is a negative temperature gradient very near the floor and the minimum air temperature measured at these positions in the room always occurs at the second thermocouple position above the floor (90 mm). Correspondingly, the maximum temperature always occurs in the zone 100 mm below the ceiling. There are, however, some notable variations in the profile shapes between these two points.

Comparison of these temperature profiles shows the maximum temperature in the room increasing with load for a given air flow rate. The air temperature just above the floor also increases with load for a given air flow rate. Some correlation between the wall and air temperatures can also be observed. The wall temperature gradients are generally less than those measured in the air, and the air-to-wall temperature differences change sign at approximately 2.2 m. In other words, heat flow from the wall can be expected to be a heat gain in the lower part of the room and a heat loss in the upper part. This is consistent with the two-zone approach to modelling such systems taken by Mundt [43] in which the vertical surfaces are divided into upper and lower halves.

A distinctive feature of room air temperature profiles in displacement ventilation systems is that the temperature just above the floor (T_{fla})—apart from very close to the supply diffuser—is

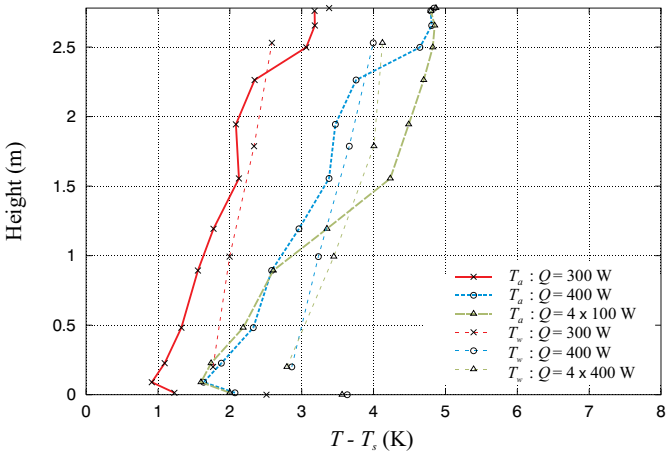

Figure 5: Air (T_a) and wall surface temperature (T_w) distributions for displacement ventilation under different heat gain conditions (Q=100–300 W) and an air change rate of 3.0 per hour.

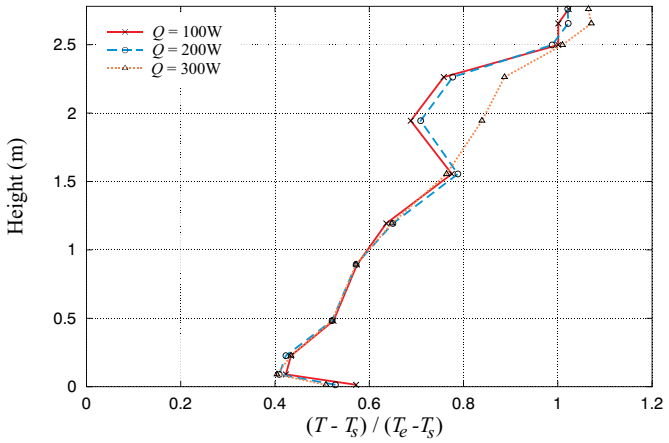

Figure 6: Normalized air temperature distributions for the displacement ventilation test cases with heat gains in the range 100–300 W and an air change rate of 1.5 per hour.

one or two degrees warmer than that of the supply. The size of this temperature difference is of some concern in determining the thermal comfort in the room. This temperature difference can be expressed as a proportion of the overall difference between supply (T_s) and extract (T_e) temperatures, with the ratio defined as $\kappa = (T_{fla} - T_s)/(T_e - T_s)$. Jackman [44]suggests a typical value of 0.4 but other published data, over a wide range of flow rates and external conditions, suggests a range of values between 0.25 and 0.55 [43].

Mundt [43] and Li *et al.* [45] have put forward a simple explanation for the existence of this characteristic temperature difference near the floor. The hypothesis is that the vertical heat fluxes in the room are the most significant. The ceiling surface is convectively heated by the warm air layer in the upper part of the room. The ceiling surface, by virtue of the overall temperature gradient in the room, is hotter than the floor surface and exchanges heat with it by radiation. This radiant flux at the floor is then balanced by the convective flux at the floor, producing the slight heating of the supply air as it flows across the floor. Thus the hypothesis is also that the convective fluxes at the floor and ceiling are approximately in balance with the net radiant flux between these two surfaces.

Further consideration of the minimum room air temperatures that occur just above the floor (T_{fla}) shown in Fig. 4 shows that the air temperature near the floor increases much less than near ceiling temperature as the heat gain is increased. Fig. 6 shows these same test case results with the air temperature profile normalized against the overall air temperature difference so that the lowest temperature is indicative of the ratio κ. With the temperature normalized in this way, the temperature near the floor is shown to be nearly the same in each case such that the ratio κ is approximately 0.4. The normalized temperature gradient in the 0.1–1.6 m zone is also very nearly the same in each case.

A similar normalized plot of the air temperature profiles for the displacement ventilation cases where the air change rate is 3.0 per hour is shown in Fig. 7. There is more variation in the shape of the temperature profiles in these cases and the ratio κ is close to 0.35. These results together suggest then, that the ratio κ is dependent on air change rate but independent of internal heat gain. This result is predicted by the three and four node models of displacement ventilation by Mundt [43] and Li *et al.* [45].

The results for the cases with the lowest heat loads (100 W and 200 W in Figs. 4 and 6) show some different features in the temperature profile in the upper part of the room (1.5–2.5 m) compared to cases with higher heat loads. In particular, there is a reversal in the temperature gradient between 1.5 and 2.0 m and also a significant step increase in temperature between 2.3 m and 2.5 m. The latter feature suggests a more pronounced sharply defined layer of warm air near the ceiling and also a higher stationary front height. This is consistent with plume ventilation theory [23] which indicates that, as plume flow rates are proportional to the third power of the heat gain, higher stationary front heights will occur at lower heat gains for a given room ventilation rate. The reversal in temperature gradient between 1.5 m and 2.0 m is more difficult to explain other than to say that there is some horizontal flow around the plumes that may introduce cooler air at this height. The plumes, in these cases, also have a weaker effect on the overall flow pattern and some local effects may affect conditions between the plumes at the sensor location. This feature, although not completely absent, is insignificant in cases with higher heat loads.

Two of the cases presented in Fig. 7 have total heat loads of 400 W. In one case this is provided from a single source and in the other by four 100W sources. The temperature profile in the latter cases suggests a deeper layer of mixed air in the upper part of the room. This is consistent with the fact that, according to plume theory, the volume of air entrained by a plume is proportional to the one-third power of the heat load. Hence, at any given height, the flow in four plumes could be expected to be 2.56 times that in a corresponding single plume.

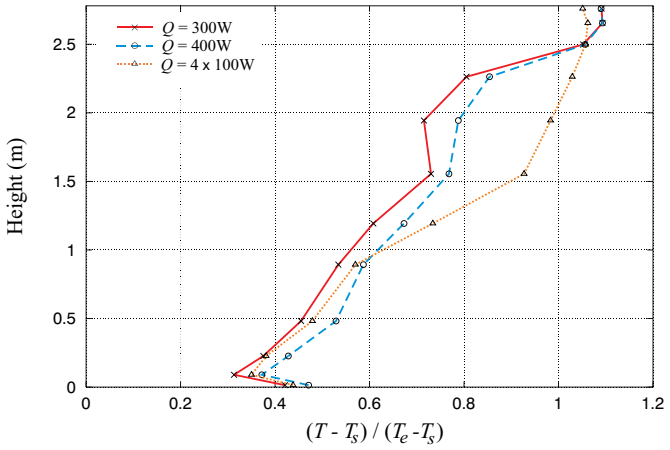

Figure 7: Normalized air temperature distributions for the displacement ventilation test cases with heat gains in the range 100–300 W and an air change rate of 1.5 per hour.

4. Displacement Ventilation and Chilled Ceiling Characteristics

The experimental results where the displacement ventilation system was operated in conjunction with the chilled ceiling are firstly presented for cases where the load and air change rate was constant but the chilled ceiling temperature was varied. Air temperature profiles for the cases where the load was 800 W (equivalent to 48 W/m^2) are presented in Fig. 8. Air and surface temperature profiles for cases where the load was 450 W (26.8 W/m^2) and 600 W (35.8 W/m^2) are shown in Fig. 9.

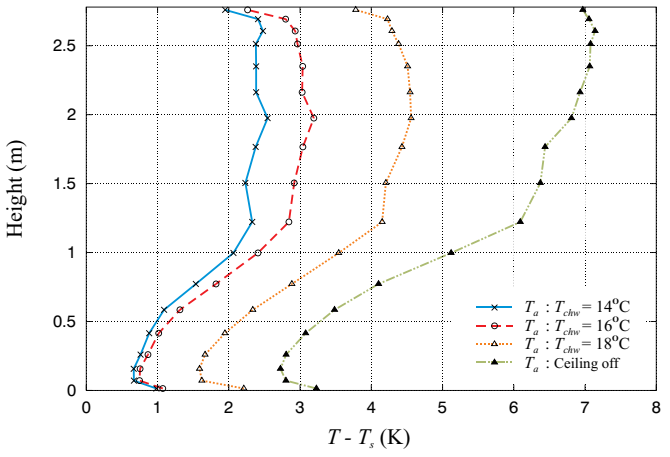

Figure 8: Air temperature (T_a) distributions for a range of ceiling chilled water temperatures (T_{chw}) and with displacement ventilation alone. The load is 800 W and the air change rate 3.0 per hour.

A number of trends are observable from the air and wall temperature profiles measured with the chilled ceiling in operation. Fig. 8 shows the reduction in maximum air temperature as the ceiling temperature is reduced whilst the other boundary conditions were kept constant. The absolute value of the vertical temperature gradient also reduces as more heat gain is absorbed by the ceiling and less by the air.

Under the experimental boundary conditions used here, the ventilation system still provides a noticeable proportion of the total cooling. This can be seen from Fig. 9, in that the maximum air temperatures increase at higher loads for the same ceiling temperatures. The wall temperatures are higher than the air temperatures in the lower part of the room—as in the displacement ventilation measurements—but are little different from the air temperatures in the upper part of the room.

In general, much more distinct negative temperature gradients were measured immediately below the ceiling than in the displacement ventilation cases. This is indicative of the convective cooling effect of the chilled ceiling panels. In a similar manner to the displacement ventilation cases, the minimum air temperatures measured in each profile occur just above the floor. Despite the addition of radiant cooling, these temperatures were found to be always higher than the supply air temperature.

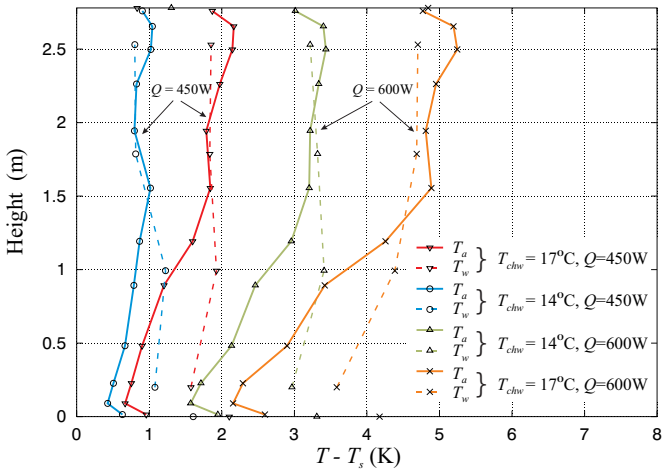

Figure 9: Air (T_a) and wall surface temperature (T_w) distributions for ceiling chilled water temperatures (T_{chw}) of 14°C and 17°C and heat gains of 450 W and 600 W. The air change rate was 3.0 per hour in these cases.

A significant difference between the displacement ventilation test cases and those with the chilled ceiling operating is in the difference between the ceiling and floor temperatures. The sign of this temperature difference is in fact reversed, being in the range -0.4 K to -3.1 K. In the displacement ventilation test cases, the ceiling surface was always warmer than the floor, so that the expected dominant radiant flux was from the ceiling to the floor. In the cases with the ceiling system operating the situation is, perhaps unsurprisingly, reversed.

In view of the ceiling surface being generally cooler than the floor, one might expect the dominant net radiant flux to be upwards from the floor to the ceiling. However, it has already been noted that in all the experiments the air temperature just above the floor was still greater than the air supply temperature. This indicates convective heat transfer from the floor to the air above, as in the displacement ventilation cases. Again, this convective flux must mainly be balanced by a net radiant flux to the floor surface as the temperature difference between the floor surface and the floor void was very small.

In order to investigate the nature of the radiant heat bal-

ance in more detail, measurements were made with a hand-held radiometer at a number of points on each room surface and around the heat sources. A numerical radiant exchange model was also constructed, in which the heat sources and tables were included in detail (details of the numerical model are given in [40]). From both the measured and calculated fluxes, it was apparent that the net radiant flux at the ceiling was approximately four times the magnitude of the net flux at the floor. This is in contrast to the displacement ventilation cases where these fluxes were approximately equal. This suggests that much of the radiant load is absorbed directly at the ceiling. This may be due to the presence of four heat sources and tables, rather than one in the displacement ventilation experiments (Fig.3). The larger plan area of the heat sources and tables has the effect of increasing the view factor between the heat sources and the ceiling and decreasing the view factor between the ceiling and the floor. Although the ceiling is cooler than the floor there is a net heating flux into the floor. This must be due to radiant coupling between the surfaces in the lower part of the room and the heat sources—the bottom surface of the tables being noticeably warm.

For one of the displacement ventilation and chilled ceiling test cases, the air temperature distribution was measured at a number of positions along the length of the room with the aim of detecting lateral temperature variations. The heat gain in this test case was 1200 W (equivalent to 72 W/m^2) and the air change rate 5.0 per hour. This was the maximum heat gain tested and the supply air flow rate was corresponding increased to maintain realistic maximum air temperatures. These measurements are plotted in Fig.10, where the dimension x is the horizontal distance along the centerline from the wall with the supply diffuser mounted on it. Position E is between one of the heat loads and the north wall, as illustrated in Fig.4.

It can be seen from Fig. 10 that the lateral variations in room temperature are confined to distinct levels in the room. Firstly, the temperature up to 0.4 m above the floor increases with distance from the diffuser, with the largest temperature difference between 0.7 m and 1.5 m from the wall. Between 0.4 m and 1.0 m height, the profile at each position is remarkably similar and has a linear gradient of approximately 3 K/m. Above the 1.0 m level there is a notable change in temperature gradient so that the profile is nearly vertical. Finally, there is a strong negative temperature gradient near the ceiling, indicative of convective cooling at the ceiling. The temperature profile measured near the wall (position E) varies little from that along the centerline of the room. Very similar profiles for cases with several heat sources and cold ceilings measured in the same chamber were reported by Taki *et al.* [46].

Consideration of the temperature profiles for the displacement ventilation and chilled ceiling test cases (Figs. 8–10) reveals rather different trends than the cases of displacement ventilation alone (Figs. 4–7). Much of the temperature rise in the room air appears to take place in the lower part of the room, over the height 0.15–1.0 m where the temperature rise is nearly linear with height. From a height of approximately 1.2 m up to 2.6 m, the temperature profiles become very similar, with only a small positive temperature gradient. The combination of these

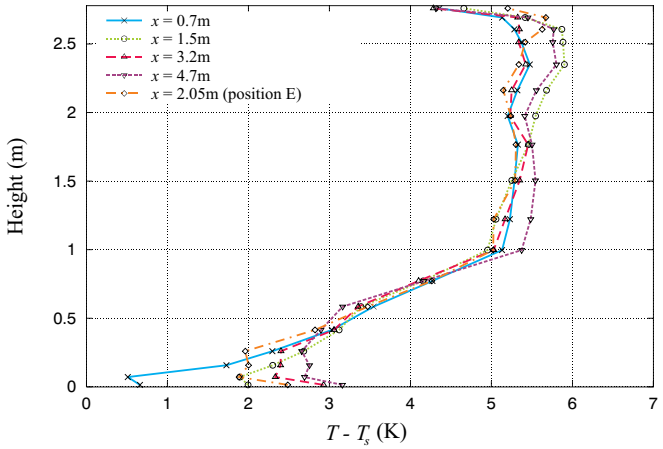

Figure 10: Air temperature distributions measured at different horizontal positions. The ceiling chilled water temperature was 16°C, the heat gain was 1200 W and the air change rate 5.0 per hour.

two features results in a 'kink' in the temperature profiles of the displacement ventilation and chilled ceiling test cases at approximately 1.2 m (1.0 m only in Fig. 10) where the gradient changes significantly.

Much of the temperature rise in the room air takes place below a height of 1.0 m; this is essentially the zone below the position of the heat sources in these experiments. This is also the region where the greatest differences between wall surface and adjacent air temperature occur—these differences being very small in the upper part of the room (Figs. 4, 5 and 9). This significant temperature rise can be accounted for by two possible mechanisms. The heat associated with this temperature rise can be either conducted from the layer of warm air above (sustained by the heat sources) or convected from the surrounding wall surfaces.

The feasibility of these two possibilities can be examined by considering the order of magnitude of the potential conducted and convective heat fluxes. It seems reasonable to assume all the supply air must flow vertically over this height range, i.e. there is vertical plug flow below the plumes. If the typical temperature increase over this height range is taken to be 1.5 K (from the measurements), an air flow rate equivalent to 3.0 air changes per hour would require a heat input of 70 W to sustain this temperature difference. The heat flow by conduction, with this same temperature difference, from the zone above is calculated to be less than 1.0 W (i.e. two orders of magnitude smaller). To consider the potential convective flux it is first noted that the wall surfaces are of order 1.0 K warmer than the air in the lower part of the room (Fig. 9). Given this driving temperature difference over the lower part of the walls, the value of the convection coefficient required to produce the estimated 70 W heat input is ~3.3 W/m^2.K, which is certainly of the expected order of magnitude for room conditions. It seems likely then, that it is convection from the walls that drives the temperature increases in the lower part of the room.

5. Room air flow and mixing processes

A simple analysis of the mass balances in the plumes and the surroundings shows that there should be a height above the base of the plumes at which the flow in the plumes is equal to the room ventilation flow. This marks the so-called stationary front. Application of plume theory indicates that the room will be divided into a lower region where the air is similar to the supply condition and an upper region above the stationary front that is well mixed warm air [23]. The height of the stationary front and thickness of this upper region are dependent on the plume entrainment rate and hence on the number of plumes and the heights of their bases. For optimum air quality, the upper mixed region should be above the occupied zone.

In these experiments, a clearly defined lower region where there is a relatively linear increase in room air temperature with height has been observed in cases both with and without the chilled ceiling operating. There is a wider variation in the temperature profiles of the upper regions of the room. It is only in the case of displacement ventilation with small single heat sources that there is an identifiable thin layer of warm air near the ceiling (Fig. 6). In cases with moderate loads, the temperature varies linearly over much of the upper region but with a reduced gradient compared to the lower part of the room (Fig. 9). This is also the case in much of the published experimental data ([10, 18, 20]. In cases with the highest loads and coolest ceilings, there is almost no temperature gradient in the upper region of the room (Figs. 8–10). This suggests much of the upper part of the room is well mixed.

Measurements of room air velocity are presented for different horizontal positions in Fig. 11. These measurements were made at the same time and at the same positions (along the room but outside the plumes) as the temperature measurements presented in Fig. 10.

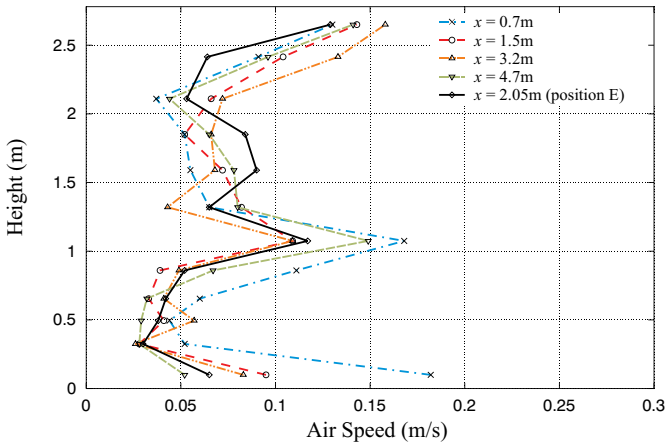

Figure 11: Velocity measurements measured at different horizontal positions. The ceiling chilled water temperature was 16°C, the heat gain was 1200 W and the air change rate 5.0 per hour (as in Fig. 10).

There are a number of features in the velocity profiles that are repeated at each of the measuring positions. It is worth noting that the velocities are all relatively low, being less than 0.2 m/s and so not a cause for concern with respect to sensations of draft. In the zone nearest the floor (0.1 m sensor height) the velocity is at a local maximum. This velocity is largest near the supply diffuser and reduces further away. In the zone above this (sensor heights of 0.33–0.86 m) the velocity falls to approximately 0.04 m/s and this is a value consistent with horizontal piston flow over this height range. (Velocities corresponding to vertical piston flow are an order of magnitude lower.) There is a similar zone, with little air movement, in the upper part of the room (sensor heights 1.32–2.11m) where the velocity is approximately 0.07 m/s. The two sensors near the ceiling indicate higher velocities, with values in the range 0.13–0.16 m/s close to the ceiling. There is another distinctive maximum, with measurements in the range 0.11–0.17 m/s at a height of 1.08 m.

The measurement of local maxima in the air velocity at the floor and ceiling could be expected in view of the flow of supply air over the floor and the spreading of the air from the top of the plumes across the ceiling. The velocity measured at the sensor closest to the ceiling, in contrast to that measured near the floor, varies little with horizontal position. The velocity further away from the center of the plumes and near the wall (position E) is only slightly reduced from that at the center of the four plumes (0.13m/s as opposed to 0.16m/s). Richardson Number (Ri) is a useful non-dimensional indicator of the nature of the convective processes and indicates the ratio of natural convection to forced convection ($Ri = Gr/Re^2$). Values in the range 0.1–10.0 indicate a mixed convection regime and values less than 0.1 suggest forced convection is dominant and natural convection insignificant. Values greater that 10.0 indicate purely natural convection. It is instructive to use the velocity measurements taken near the ceiling along with the air and surface temperature data to calculate local Richardson Number values. Values calculated at the sensor positions closest to the ceiling and over the whole range of temperature differences measured, were between 0.09 and 0.52. This therefore suggests convection heat transfer conditions near the ceiling surface are mixed but tend towards forced convection and that natural convection forces are relatively weak. Values near the upper wall surfaces were much lower as the surface-air temperature differences are correspondingly lower than at the chilled ceiling surface.

The measurement of a local maximum in the velocities near the 1.0m level is interesting as this height must be close to the height of the base of the plumes. As the sensors are omnidirectional, the flow direction at this level could not be determined directly. A simple visualization experiment was conducted by introducing neutrally buoyant smoke through the diffuser and inside the heat sources. In these visualisation experiments air movement from the supply diffuser and in the plumes was clearly visible. Air above the base of the plumes was relatively well mixed with a more stagnant zone below. Visualization of smoke added at the base of the plumes showed that the momentum of the plumes when they impinge on the ceiling is significant, so that fluid flowing from the plumes across the ceiling still has noticeable momentum as it reaches the wall and starts to flow down the wall. It is certainly not the case that the air becomes stagnant near the ceiling surface.

A well-defined gravity current could be observed flowing from the diffuser and across the floor approximately 150 mm

thick and some reversed flow immediately above this. Hence flow in the lowest part of the room was verified to be horizontal and no vertical wall currents could be observed. The direction of bulk flow near the 1.0m level was not clearly observable as the velocity was very low. However, below this height, a zone of relatively clearer air (less well mixed) was observed. This latter zone seems to correspond to the zone with the very low velocity measurements discussed above (sensor heights of 0.33–0.86 m). Since there is some separation of the fluid between this low level zone and the levels above, it seems reasonable to assume that the direction of the higher speed air motion detected at sensor height 1.08 m is lateral rather than vertical. This height is very close to the height of the top of the load simulator boxes (the base is at table top height, 0.72 m, and the top is at 1.12 m).

To test the hypothesis that the lower extent of the mixed zone in the upper part of the room is determined by the height of the base of the plumes, a further experiment was performed. In this experiment, the tables and heat sources (800 W in total) were moved to higher and lower positions (load simulator tops at 1.55 m and 0.69 m respectively). The conditions were otherwise identical. The results of this experiment are shown in Fig. 12. Where the heat sources have been raised, the changes in the temperature profile are modest. This suggests little change in the nature of the flow below the height of the heat source. The fact that there is a greater change in temperature between 2 m and 2.5 m suggests a thinner layer of warm well-mixed air close to the ceiling. Where the heat sources were lowered it can be seen that the lower limit of the mixed zone is correspondingly lowered. There is therefore a strong correlation between the vertical position of the heat source, in these test cases, and the extent of the mixed region above. In the case with the heat sources at the lower position, it is also interesting that the floor temperature is relatively higher. The ratio κ varies between 0.39 and 0.51 in these tests. This is presumably because of the changes in radiant coupling between the heat sources and the floor.

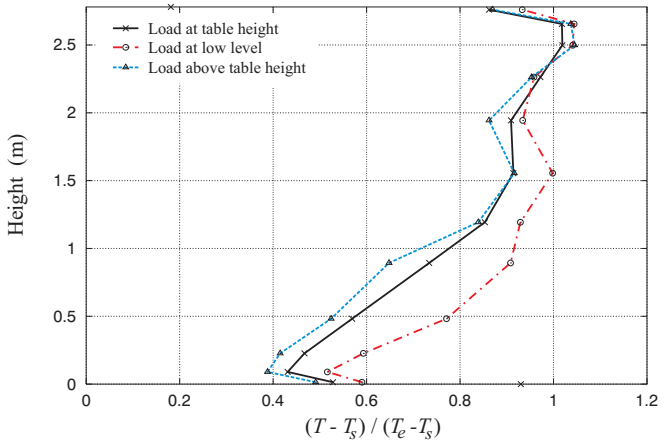

Figure 12: Normalized air temperature distributions with the heat sources at different vertical positions. In each case the air change rate was 3.0 per hour, the load 800 W and the chilled water temperature 16°C

The experimental velocity observations are consistent with the results of related CFD studies of the same conditions. Complete details of the numerical method and results can be found in [39] and a sample of the numerical data is reproduced here in Fig. 13. These results indicate that the flow in the plumes is large in relation to the room ventilation rate such that air can only be entrained into the base of the plume by being drawn from the upper region and recirculated. In this visualization the velocities in the region below the heat sources can also be seen to be relatively small. We conclude that the increased velocities at 1.0m are due to lateral flow into the base of the plumes. It can also be seen that the momentum of the plumes is significant enough to produce a relatively well-defined wall jet across the ceiling and also down the walls. The highest velocities in the recirculating zone appear to be near the surfaces and near the base of the plumes. Flow near the center of the room—between the plumes and away from the walls—is relatively still. This is the region where the velocity measurements were made.

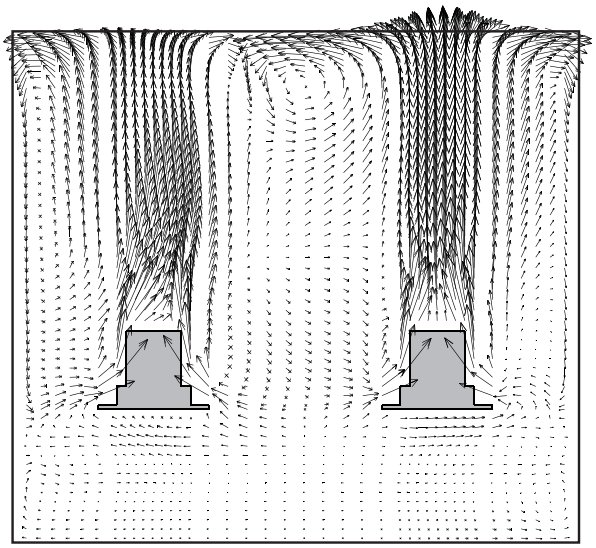

Figure 13: Calculated air velocity vectors at a cross section through two of the heat sources (x = 3.65 m). The ceiling chilled water temperature was 16°C, the heat gain was 1200 W and the air change rate 5.0 per hour (as in Fig. 10 and 11). From Rees *et al.* [39].

There are two possible contributory driving forces that may work to increase the degree of mixing in the upper zone, above that present in the displacement ventilation cases. These are the additional momentum of the plumes associated with the more powerful and more numerous heat sources, and the additional negative buoyancy given to the air near the ceiling by the convective action of the chilled ceiling panels and possibly the adjacent upper wall surfaces. It has already been noted that Ri values at these surfaces are relatively low. To further investigate the significance of these two driving forces, the temperature profiles of some displacement ventilation and chilled ceiling test cases can be compared with those of displacement ventilation test cases under similar load and flow conditions (i.e. similar conditions but with the chilled ceiling system off).

The non-dimensional temperature profiles of cases which have higher loads of 800 W (equivalent to 48 W/m^2) and supply air flow rates equivalent to 3.0 air changes per hour, are compared in Fig. 14. This is the same set of data as that in Fig. 8 but presented in a normalized manner. It can be seen that, at this level of heat gain, the change in the temperature profile at 1.2 m is distinct, both when the chilled ceiling is on and when it is off. The effect of the reduced ceiling temperature is evident in the zone extending to 0.5 m below the ceiling, where the temperature gradient becomes negative at lower ceiling temperatures.

The flow conditions in each of the four cases compared in Fig. 14 are the same. The plume entrainment processes and overall plume momentum must be similar as these are determined only by the plume strength and room ventilation rate. Although the proportion of the cooling provided by the ceiling and the absolute temperatures differ according to chilled ceiling temperature (Fig. 8), the nature of the temperature gradient and corresponding mixing processes appear to be the same. Although we cannot say that the greater air-ceiling temperature differences at lower chilled water temperatures make no difference, it seems that any such effect is of secondary significance.

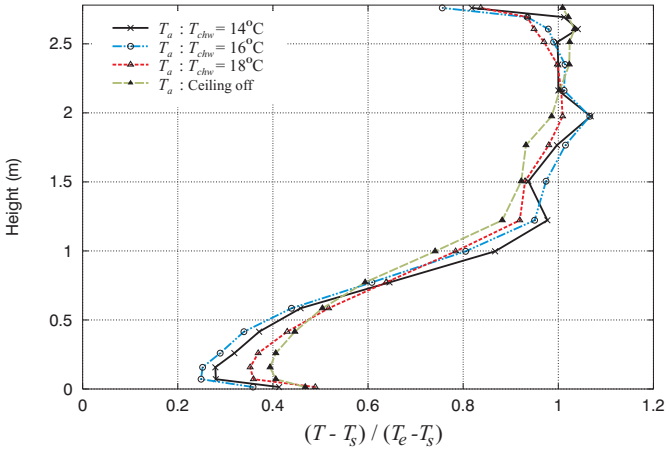

Figure 14: Normalized air temperature distributions for test cases with heat gains of 800 W, air change rate of 3.0 per hour and varying chilled water temperatures and compared to displacement ventilation alone.

Of the possible causes of enhanced mixing suggested by Behne [18] and enumerated earlier, conditions in these tests seem to be characterized by the third possibility; that significant recirculation takes place because the flow in the plumes is large in relation to the room supply. This is in spite of the experimental supply air change rate being relatively high (5.0 air changes per hour). The other causes suggested can be dismissed due to the relatively low Ri numbers measured at the ceiling and the fact that temperature measurements show no particular local cooling effects near the top of the wall due to radiant coupling with the ceiling. This latter observation also relates to an assumption made in some models of such systems that wall natural convection flows and convection coefficients can be determined from local wall-air temperature differences (i.e. purely natural convection) as in the model reported by Ayoub *et al.* [47]. In this case, although small temperature differences of this type existed, forced convection predominated at the edge of the ceiling and top of the wall. Wall convection could not therefore be defined independently of ceiling flow conditions.

In general, conditions at the ceiling and the upper region of the room seem complex and not defined by the proportioning of the load between the air and chilled ceiling systems or by consideration of the flow and temperature differences alone. The nature of the plumes and the scale of the room may play a factor in determining the momentum of the flow across the ceiling as it approaches the walls or interacts with adjacent plumes. The conditions reported here seem representative of practical office applications in being measured in a room with a ceiling at a level typical of commercial offices and at moderately high heat gain levels. It is conceivable that in taller spaces or where loads are more distributed convection and mixing conditions may be different.

Whether the mixing noticeable in these experiments corresponds to poorer air quality in the breathing zone of occupants is not clear. It is apparent from the work with breathing manikins by Rim and others [30] that the quality of inhaled air is dependent on the vertical boundary layer flow over the body and so can not simply be judged by the air quality at the same height adjacent to the body. Just as mixing is related to plume flow rates, comfort and air quality conditions may be different under part-load cooling conditions and so it would be of practical interest to examine some intermediate load and transient situations.

6. Conclusions

A series of test chamber experiments has been conducted in which a displacement ventilation and chilled ceiling system was operated under a range of steady-state conditions. Air and surface temperature measurements, along with velocity measurements, have been presented that show how the behavior of such systems depends on the operating conditions.

The thermal characteristics in the lower part of the room were found to be similar with and without the operation of the chilled ceiling. The convective fluxes at the floor were found consistently to heat the air flowing across the floor from the supply diffuser. These convective fluxes are balanced by net radiant fluxes from the ceiling in the case of displacement ventilation. Even though the ceiling temperature is reduced relative to the floor temperature when the chilled ceiling is in operation, the air temperature near the floor has been found to be greater than the supply temperature in all cases. Investigation of the radiant environment showed this was due to the radiant coupling between the heat sources and the floor. It was found that the presence of more heat loads and associated furniture in the simulated office increased the complexity of the radiant environment so that the floor and ceiling were not as directly coupled as when displacement ventilation alone was used, with fewer heat sources. A nearly linear temperature increase up to a height of approximately one meter was observed and this is most likely due to convective fluxes from the lower part of the walls.

The normalized floor air temperature ratio (κ) was found to decrease with increasing supply air flow rate and to be independent of the load size in the displacement ventilation cases. This is consistent with nodal models of displacement ventilation (e.g. [45] and [43]) that are based on the assumption that the characteristics are dependent mainly on the convective heat transfer at the floor and ceiling and the radiant coupling of these surfaces. A wider variation in this ratio was found for the chilled ceiling test cases as the radiant environment was also dependent on ceiling temperature. As previous results have indicated [21], reduction of the ceiling temperature in the chilled ceiling experiments caused a reduction in the proportion of the load transferred to the air stream and a reduction in the overall air temperature gradient in the room. As in displacement ventilation, overall air temperature gradients were found to reduce with increasing supply air flow rates.

In the displacement ventilation experiments with smaller loads, the temperature profile suggests a relatively shallow layer of warm air below the ceiling. At moderate loads, the temperature profile was nearly linear. At higher loads and/or a greater number of plumes, the temperature gradient in the upper part of the room was observed to be considerably smaller, suggesting greater mixing of the room air. The height at which the temperature gradient became smaller was found to correspond to the mid-height of the desk-mounted heat sources. It would be useful in future work to investigate a wider variety of forms of heat source, including occupants but also newer forms of office computer equipment.

Greater mixing was evident in the upper part of the room in all the chilled ceiling results, indicated by reduced temperature gradients above a height corresponding to that of the base of the plumes. Visualization experiments indicated that with greater heat gains (number of sources) the plumes have sufficient momentum to drive flow across the ceiling surface and down the walls. Consideration of the Richardson Number calculated using the velocity data has shown that convection conditions at the ceiling are predominantly forced rather than natural convection. Velocity measurements and related numerical studies have shown the entrainment of air required to sustain the plumes requires circulation of air within the upper room and occupied space to near the base of the heat sources. Comparison of the temperature gradients with high internal gains (72 W/m^2) and a range of ceiling temperatures also indicates that the recirculation and mixing in the upper part of the room is due to the momentum of the plumes and the horizontal flow resulting from their impingement on the ceiling. Any effect of reduced ceiling temperature on the degree of mixing and the temperature gradient was shown to be of secondary importance. We conclude that the fact that there is greater mixing in this type of office displacement ventilation and chilled ceiling system when compared to a purely displacement ventilation system, is not that the ceiling surface cools the air *per se*, but that such systems are operated with greater internal gains and are hence associated with stronger plume sources.

This experimental study has highlighted the complexity of the mixing processes in the upper part of the rooms with displacement ventilation and the fact that the momentum of the plumes and their impingement on the ceiling can have significant effects on the degree of mixing and the heat transfer at the ceiling surface. Although there are a number of studies of plume development that have been published (e.g. [29, 30]) little attention has been paid to impingement at the ceiling surface. Our study has also highlighted the complexity of the radiant exchange in office environments where furniture and heat sources significantly change the radiant heat balance compared to a similar empty room. We believe these topics are worthy of further study.

7. References

1. Svensson A. Nordic experiences of displacement ventilation. *Transactions of the American Society of Heating Refrigeration and Air Conditioning Engineers* 1989;95(2):1013–1017.
2. Sandberg M., Blomqvist C. Displacement ventilation in office rooms. *Transactions of the American Society of Heating Refrigeration and Air Conditioning Engineers* 1989;95(2):1041–1049.
3. Riffat S.B., Zhao X., Doherty P.S. Review of research into and application of chilled ceilings and displacement ventilation systems in Europe. *International Journal of Energy Research* 2004;28:257–286.
4. Baker M. Removal of internal radiation by cooling panels. *Transaction of the American Society of Heating & Ventilating Engineers* 1950;56:141–156.
5. Appleby P. A ceiling for cooling. *Building Services, The CIBSE Journal* 1988;10(7):57–59.
6. Kilkis B. Radiant ceiling cooling with solar energy: Fundamentals, modeling, and a case design. *Transactions of the American Society of Heating Refrigeration and Air Conditioning Engineers* 1993;99(2):521–533.
7. Feustel H., Stetiu C. Hydronic radiant cooling – preliminary assessment. *Energy and Buildings* 1995;22:193–205.
8. Alamdari F., Butler D., Grigg P., Shaw M. Chilled ceilings and displacement ventilation. *Renewable Energy* 1998;15(1–4):300 – 305. doi:10.1016/S0960-1481(98)00177-3.
9. Laine T. Cool ceiling system: for better control of office building indoor climate. In: *Proceedings of 'Indoor Air '93', Helsinki, Finland.*; vol. 5. 1993:423–430.
10. Novoselac A., Srebric J. A critical review on the performance and design of combined cooled ceiling and displacement ventilation systems. *Energy and Buildings* 2002;34(5):497 – 509. doi:10.1016/S0378-7788(01)00134-7.
11. Chen Q., Glicksman L. System performance evaluation and design guidelines for displacement ventilation. Atlanta, GA, USA: American Society of Heating, Refrigerating and Air-Conditioning Engineers; 2003.
12. Keblawi A., Ghaddar N., Ghali K., Jensen L. Chilled ceiling displacement ventilation design charts correlations to employ in optimized system operation for feasible load ranges. *Energy and Buildings* 2009;41(11):1155 – 1164. doi:10.1016/j.enbuild.2009.05.009.
13. Sandberg M., Holmberg S. Spread of supply air from low-velocity air terminals. In: *Proceedings of 'ROOMVENT-90', Oslo, Norway.* 1990:.
14. Magnier L., Zmeureanu R., Derome D. Experimental assessment of the velocity and temperature distribution in an indoor displacement ventilation jet. *Building and Environment* 2012;47(0):150 – 160. doi:10.1016/j.buildenv.2011.07.029.
15. Skåret E. Displacement ventilation. In: *Proceedings of 'ROOMVENT-87', Stockholm, Sweden.*; vol. 4a. 1987:.
16. Xing H., Awbi H.B. Measurement and calculation of the neutral height in a room with displacement ventilation. *Building and Environment* 2002;37(10):961 – 967. doi:10.1016/S0360-1323(01)00079-8.
17. ASHRAE Standard 55:2004 Thermal Environment Conditions for Human Occupancy. Atlanta, GA, USA: American Society of Heating Refrigeration and Air-conditioning Engineers Inc.; 2004.
18. Behne M. Indoor air quality in rooms with cooled ceilings.: Mixing ventilation or rather displacement ventilation? *Energy and Buildings* 1999;30(2):155 – 166. doi:10.1016/S0378-7788(98)00083-8.
19. Behne M. The influence of the arrangement of cooling ceilings on ther-

mal comfort. In: *Proceedings of 'Indoor Air '93', Helsinki, Finland.*; vol. 5. 1993:413–418.
20. Krühne H. Effect of cooled ceilings in rooms with displacement ventilation on the air quality. In: *Proceedings of 'Indoor Air '93', Helsinki, Finland.*; vol. 5. 1993:395–400.
21. Külpmann R. Thermal comfort and air quality in rooms with cooled ceilings - results of scientific investigations. *Transactions of the American Society of Heating Refrigeration and Air Conditioning Engineers* 1993;99(2):488–502.
22. Hunt G., Kaye N. Pollutant flushing with natural displacement ventilation. *Building and Environment* 2006;41(9):1190 – 1197. doi:10.1016/j.buildenv.2005.04.022.
23. Linden P., Lane-Serff G., Smeed D. Emptying filling boxes: the fluid mechanics of natural ventilation. *Journal of Fluid Mechanics* 1990;212:309–335.
24. Kaye N., Flynn M., Cook M., Ji Y. The role of diffusion on the interface thickness in a ventilated filling box. *Journal of Fluid Mechanics* 2010;652:195–205.
25. Kaye N., Hunt G. Heat source modelling and natural ventilation efficiency. *Building and Environment* 2007;42(4):1624 – 1631. doi:10.1016/j.buildenv.2006.02.005.
26. Faure X., Roux N.L. Time dependent flows in displacement ventilation considering the volume envelope heat transfers. *Building and Environment* 2012;50(0):221 – 230. doi:10.1016/j.buildenv.2011.11.007.
27. Castillo J., Tovar R. Transient cooling of a room with a chilled ceiling. *Solar Energy* 2012;86(4):1029 – 1036. doi:10.1016/j.solener.2011.06.026.
28. Zukowska D., Popiolek Z., Melikov A. Determination of the integral characteristics of an asymmetrical thermal plume from air speed/velocity and temperature measurements. *Experimental Thermal and Fluid Science* 2010;34(8):1205 – 1216. doi:10.1016/j.expthermflusci.2010.04.009.
29. Zukowska D., Melikov A., Popiolek Z. Impact of personal factors and furniture arrangement on the thermal plume above a sitting occupant. *Building and Environment* 2012;49(0):104 – 116. doi:10.1016/j.buildenv.2011.09.015.
30. Rim D., Novoselac A. Transport of particulate and gaseous pollutants in the vicinity of a human body. *Building and Environment* 2009;44(9):1840 – 1849. doi:10.1016/j.buildenv.2008.12.009.
31. Novoselac A., Burley B.J., Srebric J. Development of new and validation of existing convection correlations for rooms with displacement ventilation systems. *Energy and Buildings* 2006;38(3):163 – 173. doi:10.1016/j.enbuild.2005.04.005.
32. Jeong J.W., Mumma S.A. Ceiling radiant cooling panel capacity enhanced by mixed convection in mechanically ventilated spaces. *Applied Thermal Engineering* 2003;23(18):2293 – 2306. doi:10.1016/S1359-4311(03)00211-4.
33. Karadağ R. The investigation of relation between radiative and convective heat transfer coefficients at the ceiling in a cooled ceiling room. *Energy Conversion and Management* 2009;50(1):1 – 5. doi:10.1016/j.enconman.2008.09.008.
34. Causone F., Corgnati S.P., Filippi M., Olesen B.W. Experimental evaluation of heat transfer coefficients between radiant ceiling and room. *Energy and Buildings* 2009;41(6):622 – 628. doi:10.1016/j.enbuild.2009.01.004.
35. Thomas L.P., Marino B.M., Tovar R., Castillo J. Flow generated by a thermal plume in a cooled-ceiling system. *Energy and Buildings* 2011;43(10):2727 – 2736. doi:10.1016/j.enbuild.2011.06.033.
36. Rees S., Haves P. A nodal model for displacement ventilation and chilled ceiling systems in office spaces. *Building and Environment* 2001;36(6):753 – 762. doi:10.1016/S0360-1323(00)00067-6.
37. Hodder S., Loveday D., Parsons K., Taki A. Thermal comfort in chilled ceiling and displacement ventilation environments: vertical radiant temperature asymmetry effects. *Energy and Buildings* 1998;27(2):167 – 173. doi:10.1016/S0378-7788(97)00038-8.
38. Loveday D., Parsons K., Taki A., Hodder S. Displacement ventilation environments with chilled ceilings: thermal comfort design within the context of the bs en iso7730 versus adaptive debate. *Energy and Buildings* 2002;34(6):573 – 579. doi:10.1016/S0378-7788(02)00007-5.
39. Rees S., McGuirk J., Haves P. Numerical investigation of transient buoyant flow in a room with a displacement ventilation and chilled ceiling system. *International Journal of Heat and Mass Transfer* 2001;44(16):3067 – 3080. doi:10.1016/S0017-9310(00)00348-3.
40. Rees S. Modelling of displacement ventilation and chilled ceiling systems using nodal models. Ph.D. thesis; Loughborough University; 1998.
41. Dantec 54N50 Low velocity analyzer mark II. Denmark: Dantec Electronik; 1985.
42. Loomans M. The measurement and simulation of indoor air flow. Ph.D. thesis; Technical University of Eindhoven; 1998.
43. Mundt E. The performance of displacement ventilation systems—experimental and theoretical studies. Ph.D. thesis; Royal Institute of Technology, Stockholm; 1996.
44. Jackman P.J. Displacement ventilation. In: *proc. of CIBSE national conference, Canterbury*. 1991:364–380.
45. Li Y., Sandberg M., Fuchs L. Vertical temperature profiles in rooms ventilated by displacement: Full-scale measurement and nodal modelling. *Indoor Air* 1993;(2):225–243.
46. Taki A., Jalil L., Loveday D. Experimental and computational investigation into suppressing natural convection in chilled ceiling/displacement ventilation environments. *Energy and Buildings* 2011;43(11):3082 – 3089. doi:10.1016/j.enbuild.2011.08.002.
47. Ayoub M., Ghaddar N., Ghali K. Simplified thermal model of spaces cooled with combined positive displacement ventilation and chilled ceiling system. *HVAC&R Research* 2006;12(4):1005–1030. doi:10.1080/10789669.2006.10391448.